

**The Genesis of Hurricane Julia (2010) from an African Easterly  
Wave and its Predictability**

**A Scholarly Paper in Partial Fulfillment of the Requirements for the Degree of:**

**Master of Science**

**Department of Atmospheric and Oceanic Science**

**University of Maryland, College Park**

**MR. STEFAN F. CECELSKI AND DR. DA-LIN ZHANG (ADVISOR)**

## ABSTRACT

Tropical cyclogenesis (TCG) is one of the least understood processes in tropical meteorology today. The formation of tropical depressions (TDs), which under the right conditions grow into tropical storms (TSs), has a plethora of interacting processes. Furthermore, fewer than 10 percent of African Easterly Waves (AEWs) spawn named tropical cyclones (TCs). In this study, a 78-h cloud-resolving simulation of an AEW and its transition into TC Julia during the north Atlantic 2010 hurricane season is obtained using the Weather Research and Forecasting (WRF) model. Our study focuses on understanding the evolution of the AEW, the synoptic environment and the multi-scale processes leading to the TCG of Hurricane Julia (2010). The genesis of Julia from an AEW is traceable back five days before, based on satellite and in situ observational data. TCG occurred rapidly, taking only 18 h from the AEWs costal transition to TD status. The WRF model reproduces reasonably well the track and intensity of the storm as it goes through genesis. It is found that the AEW provides a region of preferred development for convection with enhanced low-level convergence in a region of moderate vertical wind shear and sufficient low tropospheric moisture. Also aiding in genesis was the preconditioning of the lower tropospheric column via a vortex absorption that took place roughly 30 hours prior to genesis. As two low-level vortices came together, the environment became more conducive for convection, as high CAPE and theta-e air was ingested into the AEW. With the AEW providing dynamical lift, convection was able to be sustained given the low-level environment, preconditioning the tropospheric column prior to TCG. Future work includes the use of high-resolution ensemble simulations to study the genesis of the storm, including the trigger mechanism, multi-scale interactions and thermodynamic transition. The use of the WRF-LETKF (Miyoshi and Kunii 2012) will

be used to generate the ensemble members, with computational resources being provided by NASA's Discover Linux Cluster.

# Contents

<b>1</b>	<b>Introduction</b>	<b>4</b>
a	Current Understandings of TCG	5
b	Predictability of TCG	7
c	Observational Advances in TCG	8
<b>2</b>	<b>Proposed Research</b>	<b>9</b>
<b>3</b>	<b>Preliminary Results</b>	<b>10</b>
a	Why Hurricane Julia (2010)?	10
b	WRF Model Description	11
c	Observational Data	13
d	Case Description	13
1	Near-Surface Vortex Absorption and TCG Trigger	15
<b>4</b>	<b>Tasks to be Completed</b>	<b>17</b>
a	The Upper-Level Warm Core	17
b	Mesoscale Interactions Taking Place During TCG	18
c	Vortex-vortex Interaction with Hurricane Igor	19
d	Ensemble WRF Simulations	20
<b>5</b>	<b>Expected Scientific Contributions</b>	<b>22</b>
<b>6</b>	<b>Timeline of Proposed Work</b>	<b>23</b>

# 1. Introduction

Tropical cyclogenesis (TCG) is one of the least understood processes in tropical meteorology today. The formation of tropical depressions (TDs), which under the right conditions grow into tropical storms (TSs), has a plethora of interacting processes. These phenomena and processes range from easterly waves to mesoscale convective systems (MCSs) as well as cloud microphysics, aerosol and radiative processes. Moreover, NOAA/National Hurricane Center has issued 5-day forecasts of tropical cyclones (TCs) since 2003, which require the prediction of TCG far upstream, i.e., off the shore of west Africa. However, our ability to understand and predict TCG is limited due partly to the lack of high-resolution observations at the birthplace and partly to the deficiencies in current TC models. One of the major problems is that little evidence of mesoscale cyclonic rotation can be detected at the surface prior to genesis, yielding the inability to predict and probe where or when a tropical disturbance may grow into a TS. Numerous theories exist to describe the multi-scale interactions that take place during tropical cyclogenesis, but unfortunately, it has not been until recently that such theories could be validated with field campaigns and observations.

While the dynamical enigma of TCG is slowly being unraveled, much less attention has been put into understanding the predictability of genesis. This understanding is of great importance to not only research scientists but also operational forecasters. A major reason for such lacking attention is the need of a computationally efficient way to generate high-resolution ensemble members. Our ability to run a high resolution multi-ensemble member numerical modeling system is just coming into fruition, as our ever improving technology allows for greater computational power. The ability to quantify TCG with a better under-

standing of its predictability is the next step in not only better understanding TCG, but being able to forecast it as well.

*a. Current Understandings of TCG*

Previous studies have referred to TCG as a two-step problem: a) the preconditioning of the synoptic and meso- $\alpha$  environment and b) the construction and organization of a TC-scale vortex at the meso- $\beta$  scale (Wang et al. 2010a). The first step involves the general characteristics of the synoptic-scale environment being favorable, such as little vertical wind shear, warm sea surface temperatures (SSTs), sufficient column moisture content and the preexistence of a low-level cyclonic disturbance. Accompanying these criteria are the different synoptic-scale phenomena that provide dynamical lift to initiate TCG: Intertropical Convergence Zone (ITCZ) breakdowns (Kieu and Zhang 2009) in the East Pacific and African easterly waves (AEW) in the Atlantic basin (Vizy and Cook 2009). Further advancing the idea of an ideal synoptic environment is the theory of the marsupial pouch (Dunkerton et al. 2009), which revolves around the notion that the pre-depression perturbation is protected dynamically from adverse conditions such as dry air or large vertical wind shears. The marsupial pouch paradigm treats an AEW as the parent which protects the developing TC as it becomes better organized and undergoes thermodynamic transformation.

While there has been general agreement on the first step of TCG, dissenting opinions emerge for the formation of the low-level meso- $\beta$  vortex. The bottom-up and top-down hypotheses have been proposed as two of the possible processes leading to TCG. In the top-down frame of mind (Bister and Emanuel 1997; Ritchie and Holland 1997), the low-

level cyclonic circulation is an extension of a pre-existing midlevel cyclonic vortex, which may be reconstituted downward to create the surface circulation. Also within the top-down realm is the merging of two midlevel vortices within a region of already large-scale low-level cyclonic circulation. This merging can lead to a much more intense mesoscale convective vortex (MCV) that can be extended towards the surface enhancing low-level cyclonic vorticity. Bister and Emanuel (1997) suggested that precipitation and evaporative cooling below the melting level act to help advance the MCV towards the surface, enhancing the low-level cyclonic circulation. This method, however, has been shown to be ineffective in the movement of the MCV towards the surface since the downdrafts in MCSs during TCG are weak (Zisper and Gautier 1978).

Contrasting the top-down view is the bottom-up hypothesis (Zhang and Bao 1996b; Hendricks et al. 2004; Montgomery et al. 2006). This theory still uses the notion of pre-existing low-level cyclonic vorticity that is weak in the initial stages of TCG. Under favorable mesoscale and synoptic-scale conditions, the circulation is then spun up via deep convection, leading to the generation of the meso- $\beta$  cyclonic vortex. Surface-based convective elements make up the major notion of this theory, as up-scale processes (mainly localized diabatic heating and enhanced low-level convergence) invigorate the low-level cyclonic circulation and precondition the atmospheric column with sufficient column moisture. The bottom-up theory has been recently augmented by the addition of vortical hot towers (VHTs) (Hendricks et al. 2004; Montgomery et al. 2006), whose concept was revived from that of convective hot towers of Simpson et al. (1998) after finding their vortical aspect from high-resolution numerical weather prediction (NWP) models. VHTs are loosely defined as cyclonically rotating convective updrafts with a life span of around one hour and a horizontal length on

the order of 1 to 10 km. Simpson et al. (1998) showed that hot towers could contribute to TCG via the compensating subsidence outside the core of the towers, which in turn would cause hydrostatic pressure falls. On the other hand, Montgomery et al. (2006) suggested that VHTs are the building blocks of TCG; conglomerating to create and/or enhance the MCV via diabatic vortex merging. The combined effects of heating due to each VHT would then enhance the pre-existing low-level cyclonic circulation. Montgomery et al. (2006) also hypothesized that these towers would only be present in certain synoptic conditions. These include sufficient convective available potential energy (CAPE) and the presence of larger-scale low-level cyclonic vorticity.

*b. Predictability of TCG*

Fewer than 10 percent of AEWs spawn named TSs. This statistic alone depicts the troubles not only in simulating TCG, but also in predicting it with any substantial lead-time. While there have been improvements in producing forecasts of mature TCs, virtually no improvements have been made in the prediction of TCG. Much effort has been put into improving the track and intensity errors of a mature TC using ensembles, however, these methods have not been extended to TCG from AEWs operationally. Literature shows that few studies have actually investigated the predictability of genesis, with or without the use of ensemble members of some kind. As stated in previous work moist convection has the highest uncertainty at all time and spatial scales in NWP models when compared to other precipitation processes. The inability to resolve convective elements in coarse resolution models limits the skill of the simulation due to noise in the deterministic forecast. Unfortunately, the un-

derlying dynamics of TCG is cemented in moist convective processes (Hendricks et al. 2004; Montgomery et al. 2006) and thus the predictability of TCG is rooted in the predictability of moist convection. The use of ensemble members to better understand TCG has just come to the surface in the research community. Sippel and Zhang (2008) have shown from ensemble simulations that a deep moisture layer and high CAPE are the two most important factors in the ICs for TCG based on a case study of a non-developing tropical disturbance. They rationalized that these characteristics led to convective bursts occurring more rapidly, allowing for a quicker spin-up toward TCG. The use of ensemble forecasts will prove to be very useful for investigating the dynamics of TCG, including the trigger of TCG.

*c. Observational Advances in TCG*

The aforementioned hypotheses have been debated for many years, but most research on TCG has agreed on one major problem: the lack of high-resolution observational data at the birth-place (Dunkerton et al. 2009; Fu et al. 2007; Kieu and Zhang 2009). The regions in which TCs form are considered data sparse regions where in situ observations are for the most part nonexistent. Furthermore, there has been a lack of field campaigns that focus on TCG, with greater focus on mature and land-falling systems. Recently, field campaigns have taken place to further utilize aircraft, satellite data and NWP products in conjunction with other observational datasets to better understand TCG. They include the NASA-funded Genesis and Rapid Intensification Processes (GRIP) experiment, the NSF-funded Pre-Depression Investigation of Cloud-systems in the Tropics (PREDICT) project, and the NOAA-funded Intensity Forecasting Experiment 2010 (IFEX10). The observational

datasets put together by these three projects are by far the most robust seen in TCG observational studies. When combined with numerical simulations, these field campaigns will lead to a better understanding of the mechanisms surrounding TCG.

## 2. Proposed Research

For my Ph. D. thesis research, I propose to conduct a case study investigating the processes leading to and the predictability of the genesis of Hurricane Julia (2010) that occurred over North Atlantic Ocean. Hurricane Julia formed from a strong AEW that moved off the African coast in mid-September 2010. This study will employ numerous observational datasets as well as numerical simulations created by the Weather Research and Forecasting (WRF) model to investigate the following hypotheses:

- i. AEWs provide the necessary quasi-balanced forcing (i.e., upward motion and cyclonic vorticity) for the development of deep convection and rotation via stretching, given that the synoptic conditions necessary for genesis are present;
- ii. The vortex-scale surface pressure falls occur as a result of convectively generated compensating subsidence warming in the upper troposphere. This warming may increase markedly once the upper-level outflow develops, triggering TCG;
- iii. The vorticity generation that leads to TCG occurs through a bottom-up process, up-scale growth through vortex mergers and the axis-symmetric conglomeration of cyclonic vorticity associated with convectively generated vortices (i.e., VHTs);
- iv. Vortex Rossby wave energy dispersion and vortex-vortex interaction can either in-

hibit or aid in triggering TCG, depending on the distance between the two interacting storms;

- v. The initial conditions used for TCG forecasts (simulations) play an intricate role in both how well genesis and its related dynamics are predicted. Meteorological variables such as column moisture content and CAPE (as shown by Sippel and Zhang (2008)), among other convective parameters are the most important ICs in order to properly diagnose TCG and its trigger;

The coming sections will describe in-depth the WRF model, the data sets employed for the research and the methods used to test the above hypothesis.

### 3. Preliminary Results

#### *a. Why Hurricane Julia (2010)?*

The choice of Hurricane Julia for this case study was made for many reasons. First, Hurricane Julia formed from a strong AEW that is traceable back nearly five days from the time of genesis. Figure 1 shows a Hovmller diagram from September 5th to 12th, giving insight on where the AEW originated from, how it formed, and its interaction with other meteorological features before it took on tropical cyclone characteristics. It is evident from Fig. 1 that Hurricane Igor (denoted by the dashed arrow) was in close proximity to Hurricane Julia during the genesis phase. This proximity may have significant implications on the initiation of genesis and the overall synoptic environment for Hurricane Julia's formation.

Second, the genesis of Julia came as a surprise of the NHC forecasters. As noted in the

Tropical Cyclone Report: “The genesis of Julia was not well anticipated. The disturbance that became Julia was introduced into the Tropical Weather Outlook (TWO) with a medium (30 percent) change of formation only 18 h before the system became a tropical cyclone (Beven and Landsea 2010)” Furthermore, only 6 hours before the storm became a depression did the NHC finally raise the probability of genesis to 70 percent. The report goes on to state that numerous global model forecasts did successfully predict the genesis of the storm with a several day lead-time. The aforementioned statements lend substantial motivation for the choice of the storm. If the predictability of genesis was high in global-scale NWP models, why was there a lack of predictability and such a short lead-time for the forecasters? A better understanding of why and when Julia formed, both from a dynamical and predictability perspective, could directly impact how the NHC handles such genesis forecasts for future storms of similar origin.

*b. WRF Model Description*

The WRF model used for this study has been widely used in meteorological research and especially so for mesoscale investigations. For the case study, the WRF model is used to generate simulation output for examining the aforementioned hypotheses. We will use WRF-ARW (advanced research dynamic solver) model version 3.2.1 with the WRF pre-processing system (WPS) version 3.3. The control simulation for the study, which has been successfully completed, consists of three domains, two of them nested. The horizontal resolution of the three domains are 12 -4-1.33 km, respectively. The 1.33-km domain is a moving domain that follows the AEW disturbance. Figure 2 shows the domain set up with the map representing

the 12-km, outermost parent domain. The parent domain was set to be as large as possible, especially downstream of the storms track to ensure that Hurricane Igor, which appeared to have possible vortex-vortex interaction with Hurricane Julia, stayed completely within the domain. The model physics options include a) the Kain-Fritsch convective parameterization scheme for the 12- and 4-km domains; b) the Thompson microphysical scheme; and c) the YSU planetary boundary layer (PBL) parameterization. The 1.33-km domain had no convective scheme, as it was cloud resolving. All domains use 36 vertical levels, which were clustered both near the PBL and near the top of the troposphere. This vertical clustering was done to capture both the confluent motions of the lower troposphere as well as the diffuence in the upper troposphere that are prominent during the TCG stage.

The model is initialized at 0000 UTC 10 September and is integrated for 78 h, ending at 0600 UTC 13 September. The model initial and lateral boundary conditions are supplied from the ERA-Interim Analysis, which is a 6-hourly global analysis from the European Centre for Medium-Range Weather Forecasts (ECMWF). The ERA-Interim project has numerous improvements over the ERA-40 reanalysis, such as higher horizontal resolution ( $0.7^\circ$ ) and more vertical levels (from 23 to 37). The SSTs are initialized using NOAAs Daily Optimal Interpolation (OI) SST analysis version 2.0 at  $0.25^\circ$  horizontal resolution (Reynolds et al. 2007). This SST data set is created from the Advanced Very High Resolution Radiometer (AVHRR) and the Advance Microwave Scanning Radiometer (AMSR) satellite instruments and quality-controlled with in situ observations.

### *c. Observational Data*

Numerous observational data sets were obtained to investigate the synoptic conditions and to validate the WRF output. They include satellite data from METOSAT-9, GOES-EAST, and various polar orbiters. Multiple products were used from the aforementioned satellites, including visible, infrared (IR) and water vapor products. Other satellite-derived products such layer wind shear, vorticity and divergence were used for further validation of the synoptic environment.

Limited upper air data is available in the region where Julia made its transition to a TC. Three west African in situ upper air stations are of interest for the evolution of the AEW into Hurricane Julia and are Dakar (GOOY), Tambacounda (GOTT) and Niamey (DRRN).

### *d. Case Description*

To provide a synoptic overview on the genesis of Hurricane Julia, I will investigate the large-scale flow field at the following four critical stages: i) an AEW over land, ii) AEW making costal transition, iii) AEW/pre-depression vortex over water, and iv) genesis. The four stages are depicted in Fig. 3 and show the evolution of the disturbance both in observations and the WRF control simulation. For this work, the definition of TCG will refer to the time that the NHC officially declared the storm a TD.

Figure 4a compares the control simulation track to the NHC best track from 0600 UTC 10 Sept to 0600 UTC 13 Sept. Finding the storm track from the WRF simulation can be influenced by topography and as a result uses multiple products. Appendix 1 explains how the track was created and what products were used. Substantial track error exists early

in the WRF simulation but becomes better than the best track forecast error for the 48 hr forecast (WRF 48 hr forecast  $\sim 130\text{km}$ , best track 48 hr forecast  $\sim 146\text{km}$ ). The large track error early simulation could be due the best track estimate over land being strictly defined by spatial cloud patterns as defined in satellite imagery (W. Hoggsett, personal communication). This track is prone to error when circulation features are not well defined by cloud patterns (Fig.3, first critical time). Nonetheless, the WRF forecast errors are close to what the average forecast error was for the official forecast track (Rappaport and Franklin 2009; Beven and Landsea 2010), validating a reasonable simulation of the storm track.

Figure 4b compare the storm intensity, both in minimum surface central pressure ( $P_{MIN}$ , in hPa) and 10 m maximum wind speed ( $V_{MAX}$ , in  $\text{m s}^{-1}$ ) between the WRF control simulation and the NHC best track analysis. Obviously, the model-predicted  $P_{MIN}$  is excellent compared to the NHC best estimate, and similarly so for  $V_{MAX}$ . Figure 4b also depicts how slow intensification was before TCG. The storm exhibited a steady, albeit slow decrease in  $P_{MIN}$  prior to genesis at 0600 UTC 12 Sept. Deepening rates from the observed are just over  $0.1 \text{ hPa hr}^{-1}$ , signifying very weak pressure drops pre-TCG. Clearly, the potency of the strong AEW was a mid-tropospheric event with little surface inflection. This is evident in the strong circulation field in the streamline analysis found in Fig. 3.

The AEW that becomes Hurricane Julia was a strong wave with a distinct closed circulation at 700 hPa in the co-moving framework (Fig. 5). After costal transition, the disturbance develops a much more coherent structure of relative vorticity at 700 hPa that becomes co-located with a closed circulation center. The potency of the AEW was noted in Tropical Cyclone Report (Beven and Landsea 2010) and was captured at the Dakar rawinsonde station between 1200 UTC 11 and 0000 UTC 12 Sept (Fig. 6).

The large-scale environment was favorable for the formation of Julia in terms of high SSTs, a moist column and a distinct low-level cyclonic circulation. Specifically, SSTs of above 26°C progressing from the west African coast westward between 5 and 15 N allowed for sustainment of a disturbance going through TCG (Fig. 4). A significant layer of dry air associated with a Saharan Air Layer (SAL) outbreak was present to the north of Hurricane Julia during TCG. This air mass, however, did not have direct impact on TCG, as it was several hundred kilometers to the north of the TCG location. Sufficient low level column moisture is present surrounding the storm (Fig. 7), while deep convection struggles to transport this moisture into the 600-200 hPa layer. The upper column of the atmosphere does moisten closer to genesis as deep convection penetrates deeper into the layer. Shear is moderate over the AEW for both the 925-600 hPa and 600-200 hPa layers between 0000 UTC and 1200 UTC 11 Sept with the most noticeable shear in the upper levels. This bias towards the upper levels is consistent with the weaker near-surface circulation associated with the AEW, as well as the AEJ and its related shear being to the north of the storm. Furthermore, this moderate shear contests the idea that low-magnitude vertical shear is needed for TCG and supports postulations made by Dunkerton et al. (2009), which proclaim that deep layer shear might not be as detrimental to TCG as it is to mature TCs.

#### 1) NEAR-SURFACE VORTEX ABSORPTION AND TCG TRIGGER

It has widely been recognized that the trigger to TCG refers to the process by which a non-intensifying tropical disturbance transitions into a developing tropical and intensifying tropical disturbance. Intensification from a weak tropical disturbance is not an instantaneous

process, instead a response that involves environmental preconditioning and interactions between multiple spatial scales. The trigger to genesis has been theorized as being a mesoscale event (Montgomery et al. 2006) as well as a large-scale event based on sufficient column moistening (Bister and Emanuel 1997).

As the AEW moves over the Guinea Highlands between 0000 UTC and 1800 UTC September 11 two distinct near-surface circulations are present in streamline analyses at 1000 hPa (Fig. 8). These two vortexes merged off the coast with TCG taking place only 30 h after the merge occurred. The merging of these two distinct surface features, each with very different thermodynamics characteristics helped to trigger genesis.

The northern vortex (labeled 1 in Fig. 8) was a very shallow, intense thermal low with high CAPE but very low column moisture content. On the other hand, the southern vortex (labeled 2 in Fig. 8) had cooling below 700 hPa with low CAPE but high column moisture content. It is also co-located nicely with the center of the mid-level AEW circulation. The red line in Fig. 8 depicts a cross-section through both vortexes with the B representing the start of the cross-section and the E representing the end of the cross-section at 0600 UTC 11 Sept. It is evident that the northern vortex is a low-level thermal low with very strong positive temperature deviations below 2000 m, as is shown in 9. Figure 10 shows a cross-section of relative humidity (RH) through both vortexes reinforcing the idea that the northern vortex is dry, thermal low below 700 hPa with RH values below 60 percent. The southern vortex at this time is well saturated below 700 hPa with RH well exceeding 90percent for a majority of the column.

The merging of these two surface vortexes yields the development and organization of deep convection by which TCG occurred. The northern vortex provides the sufficient ther-

mododynamic energy for the sustainment of deep convection (high CAPE) while the AEW (evident through its surface inflection as the southern surface vortex) provides the dynamical lift for convective initiation. Sustained convection is evident after merging takes place with the cyclonic vorticity structure becoming more coherent shortly thereafter (Fig. 5 and Fig. 8).

## 4. Tasks to be Completed

### *a. The Upper-Level Warm Core*

Previous studies have cited a criterion for genesis as being sufficient low-level large-scale cyclonic vorticity. However, there are other methods by which low MSLP can come about within a large-scale circulation field such as an AEW. We propose the MSLP changes to the presence of an upper level warm core that is present before genesis, which has been demonstrated by (Zhang and Chen 2012). This task will investigate the idea of an upper-level warm core that lowers MSLP via hydrostatic pressure falls. Hoxit et al. (1976) have demonstrated that warming due to subsidence in the upper troposphere have contributed to the presence of meso low pressures downstream of mid-latitude mesoscale convective systems. They were able to show that surface pressure falls of  $2\text{-}4\text{ mb hr}^{-1}$  can occur with subsidence of tens of centimeters per second within the 100 hPa to 500 hPa layer. While their work demonstrated meso-low formation in a moderately sheared environment, recent work has suggested that shear might not inhibit TCG as much as previously thought (Dunkerton et al. 2009), allowing for the idea of convective detrainment and hydrostatic pressure falls in

a moderately sheared tropical environment to be plausible. The time-height evolution of the temperature difference from the initial time to the genesis time shows a distinct upper-level warm core near 9 km that forms nearly 24 h before genesis (Fig.11). We will quantify the expected hydrostatic pressure falls based on the height of and anomalies associated with the warm core as shown. This will confirm that the feature does have a feedback on MSLP pressure falls prior to and at genesis. The upper troposphere and deep layer shears will be documented to see if the warm core is displaced down shear from the surface disturbance, which would coincide with mechanisms mentioned in Hoxit et al. (1976). This shear will also give insight on how the warm core structure is maintained, since stronger shears are suspected to make the structure less coherent and as a result, less efficient in hydrostatic pressure falls at the surface. Finally, convective detrainment must be investigated in order to see how deep convection impacts the warm core. We will confirm (or deny) that the enhanced upper-level divergence produced by the convection protects the warm core structure from being destroyed, allowing for for MSLP falls to occur.

*b. Mesoscale Interactions Taking Place During TCG*

While an upper-level warm core could possibly feedback on low large-scale MSLP, it is believed that large-scale cyclonic vorticity associated with TCG is an up-scale process. To investigate the idea that cyclonic vorticity generation in TCG is a bottom-up process, we will document the time-height evolution of the large-scale cyclonic vorticity field using the 12 km simulation output. We will calculate the covariances of various meteorological parameters to see how energy and vorticity is communicated between multiple spatial scales.

The role of VHTs versus a larger-scale meso- $\beta$  complex for the generation of cyclonic vorticity will be demonstrated by the number of VHTs present and how their relative vorticity field compares in magnitude to that of the meso- $\beta$  disturbance. We will set multiple thresholds for the magnitude of relative vorticity and use these thresholds to investigate the roles meso- $\gamma$  and meso- $\beta$  disturbances in using output from the 1.33 km WRF control simulation.

*c. Vortex-vortex Interaction with Hurricane Igor*

For Task 3, we will investigate the interactions of Hurricane Julia with Hurricane Igor. As mentioned earlier, the proximity between the two storms could have significant impacts on Julias genesis (Fig.1). This task will entail looking at the Rossby wave energy dispersion from Hurricane Igor to Julia. It has been shown in past research (Li and Fu 2006) that energy from a mature tropical cyclone propagates opposite to the motion vector, which is typically to the southeast of the storm. Thus, an analysis of how energy is propagated away from Igor and what interactions it could have had for the genesis of Hurricane Julia is essential. To study such phenomena, we will conduct analysis of low-level wind and moisture fields averaged over a three-day period (a temporal average over the last 72 hours of the WRF simulation). By averaging, we will be able to capture Rossby wave-like motions, and can identify any wave patterns between Igor and Julia. We will also calculate an energy propagation vector ( $E$ ), as defined by Trenberth (1986), which describes the transfer of energy via wind perturbations on the synoptic timescale. To truly understand the role of Rossby wave energy, temporal averages greater than three days will need to be used to calculate energy propagation. As a result, ERA-Interim analysis data for up to ten days prior to Hurricane Julias genesis will be

used to calculate energy dispersion using Trenberths energy propagation vector. This allows us to isolate energy traveling at the sub-synoptic, synoptic and super-synoptic timescales which are mainly due to Rossby wave dynamics.

Another method to investigate vortex-vortex interaction will be to remove Hurricane Igor using the TC bogus program built into the WRF-ARW. This program gives the ability to remove a TC given a certain point location. Additional pre-WRF processing is done through program TC.exe, which removes the storm and rebalances the initial and boundary conditions (Frederick et al. 2009). A supplemental WRF simulation will be generated with Hurricane Igor removed using the above method. This simulation will then be compared to the control simulation to see what dynamic and thermodynamic changes occur to the TCG of Julia when TC Igor is removed.

#### *d. Ensemble WRF Simulations*

We plan to employ a newly created Local Ensemble Transform Kalman Filter (LETKF) by Miyoshi and Kunii (2012) for the WRF model. Using the LETKF code, we will produce an ensemble of initial conditions in which each member will generate a simulation of the genesis of Hurricane Julia. The WRF-LETKF has been tested by Miyoshi and Kunii (2012) for a tropical cyclone in the western Pacific using a horizontal spatial resolution of 60 km. Twenty or twenty-seven ensemble members will be run from the perturbed initial conditions generated by the LETKF. We plan to keep consistency between the control run and the ensemble members, so each ensemble member would also contain three domains with 12 km, 4 km and 1.33 km for spatial resolution. As advantageous as this may seem, Dr. Miyoshi

developed the LETKF code to be run using a Message Passing Interface (MPI) computing which takes advantage of isolating different cores for each individual ensemble run. Thus, each ensemble simulation is run separately on different processors, instead of all the members sharing the same cluster of processors.

The computational resources to be used will be the Discover linux cluster provided by NASAs High-End computing resources under the Science Mission Directorate. We have successfully obtained run time by NASAs High-End Computing (NASA HEC) for use of their linux cluster to conduct the ensemble simulations. We have requested the use of 114 processors on NASAs Discover machine for the ensemble simulations. Each processor in the Discover machine is a dual-core 3.2Ghz processor with 2GB of memory dedicated to each processor. We have also requested 4TB of disk space to hold simulation output for long-term use, with an additional 1TB for transferring data to and from University of Maryland servers.

To successfully employ the WRF-LETKF system, an additional coarse domain will be created for the LETKF cycle. This domain will be a large, 60 km horizontal resolution in which NCEP PREPBUFR and AIRS observation data will be assimilated with ERA-Interim data. The LETKF cycle will run for a period of five days prior to the initialization time of the control run at 0000 UTC September 10, allowing for proper generation of the initial conditions using the observations and the ERA-Interim data.

Upon completion of the ensemble simulations, we will investigate the ensemble mean and each individual ensemble members, especially outlying members (those that create too strong of a storm or those who never create a storm) to see how well genesis is captured using ensemble members compared to the control run. By looking at individual outlying

model solutions, we can isolate any dynamical processes that either lead to TCG or never at all. This will include investigating the difference between ensemble members for various convective parameters such as CAPE, Precipitable Water (PW), Convective Inhibition (CIN) as well as other variables (such as SSTs) through the simulation period. We will also attempt to document the trigger of TCG and how it varies between each of the members (if that member had genesis occur). This will further validate the trigger mechanism found in the preliminary results. Using methods similar in investigating the control simulation under the the preliminary results for each ensemble member and the mean, we will be able to document the differences dynamically and thermodynamically between ensemble members and ensemble mean.

## 5. Expected Scientific Contributions

Successful completion of this project will provide a new understanding on the predictability of and the multi-scale processes leading to TCG from AEWs. This better understanding involves the mechanisms by which the AEW makes a transition into a TC, what the triggers of TCG are and how sensitive a model simulation is to the ICs. The results will also help confirm the current TCG theories while demonstrating that other mechanisms might be involved in TCG. Furthermore, this study will give insight on the state of NWP with respect to TCs. A better understanding on the predictability of TCG will also be possible from this study via the use of ensembles and the LETKF system. The LETKF system could have valuable impacts on the operational use of ensembles for TCG, lengthening lead-times for forecasted storm development. In addition, this project will generate both peer-reviewed

journal publications and conference presentations.

## 6. Timeline of Proposed Work

Present – March 2012: Produce first publication on the TCG of Hurricane Julia based on preliminary results and tasks 2 and 3. Start producing ensemble members for Task 4.

March 2012 – December 2012: Finish producing ensemble members for Task 4 and start diagnostic analysis on ensemble results. Produce 2nd publication on other findings from Tasks 2 through 5. Start putting together results for Ph. D. dissertation.

December 2012 – May 2013: Finish diagnostic analysis on ensemble members and produce publication on findings. Finish and defend Ph. D. dissertation in May.

### *Acknowledgments.*

This work is supported by NASA Headquarters under the NASA Earth and Space Science Fellowship Program *Grant NNX11AP29H*.

Computational resources for this project are provided under NASA Science Mission Directorate (SMD) HEC award number *SMD-11-2455*.

The ERA-Interim data set was provided by: The Research Data Archive (RDA), which

is maintained by the Computational and Information Systems Laboratory (CISL) at the National Center for Atmospheric Research (NCAR). NCAR is sponsored by the National Science Foundation (NSF). The original data are available from the RDA (<http://dss.ucar.edu>) in data set number ds627.0.

The NOAA Optimal Interpolation SST data set was provided by:

<http://www.ncdc.noaa.gov/oa/climate/research/sst/oi-daily.php> and is created by Richard W. Reynolds and Chunying Liu, NOAA/NESDIS/NCDC in Asheville, NC.

The Satellite data sets were provided by: Cooperative Institute for Meteorological Satellite Studies (CIMSS) tropical cyclone archive maintained by the University of Wisconsin in Madison, WI and the PREDICT field catalog maintained by NCARs EOL program. The CIMISS page can be found: <http://tropic.ssec.wisc.edu/archive/> and the PREDICT field catalog: <http://catalog.eol.ucar.edu/predict/index.html>.

# APPENDIX

## Appendix 1: Creation of the WRF Simulation Track

The tracking of a tropical disturbance from an AEW is a difficult process can use many different methods, both subjective and objective. The main reason for the difficulty is the high terrain in southwest Africa called the Guinea Highlands. Terrain elevation reaches upward of 900 meters in some areas in this region. Furthermore, the region is more densely vegetated compared to other parts of Africa (ie. the Sahara Desert) due to the Niger river valley. As a result, any near surface circulation (10 m, 1000 hPa, 92 hPa) is directly impacted by the terrain, resulting in unreliable streamline analyses of AEWs. Thus, tracking a pre-TD over from land to ocean must require the use of mid-atmospheric charts over land, rather than surface charts.

There are a few methods by which AEW centers are identified. The most subjective is a human analysis that is created using a suite of products that depict the AEW at various levels. Most commonly, 925 hPa, 850 hPa and 700 hPa streamline and relative vorticity analyses are used to determine the center of the wave, as well as a Hovmller analysis depicting the relative vorticities or meridional winds over a particular amount of time at a certain level. However, previous studies have shown there is a diurnal variation in the magnitude of relative vorticity at 925 hPa, making it difficult to track weak AEWs and their associated cyclonic relative vorticity maxima. Dunkerton et al. (2009) devised a method to better identify weak

AEWs by subtracting the phase speed of the wave ( $C_p$ ) from the wind field, making the wave stationary. This is called the co-moving frame of reference, and is used to separate the mean flow field from that of the circulation associated with the AEW. This can be accomplished by calculating the storm's speed via approximate circulation center fixes over a period of time and then subtracting the vector difference to create the co-moving streamlines. A rough estimate of circulation center must be prescribed in order to get the correct phase speed, thus again relying on human means of approximating wave center.

Other research has shown that the least track errors are associated with analyzing the 850 hPa relative vorticity and streamline fields over land, as well as for weak tropical disturbances over ocean (Snyder et al. 2010). After substantial effort, this work uses a combination of 700 hPa relative vorticity and streamline fields to analyze the circulation center overland. As Julia approaches ocean, the use of lower tropospheric levels is used to track circulation center as the storm strengthens since the impact of topography is lessened and the diurnal cycle is muted. The track shown from the WRF simulation is based off of 700 hPa over land when the disturbance is an AEW and MSLP (when closed contours occur at the 2 hPa interval) over water.

## REFERENCES

- Beven, J. L. and C. L. Landsea, 2010: Tropical cyclone report hurricane julia (al122010) 12 – 20 september 2010. National Hurricane Center.
- Bister, M. and K. A. Emanuel, 1997: The genesis of hurricane guillermo: Texmex analyses and a modeling study. *Mon. Wea. Rev.*, **125**, 2662–2682.
- Dunkerton, T. J., M. T. Montgomery, and Z. Wang, 2009: Tropical cyclogenesis in a tropical wave critical layer: Easterly waves. *Atmos. Chem. Phys.*, **9**, 5587–5646.
- Frederick, S., C. Davis, D. Gill, and S. Low-Na, 2009: Bogussing of tropical cyclones in wrf version 3.1. WRF Users Workshop 2009.
- Fu, B., T. Li, M. S. Peng, and F. Weng, 2007: Analysis of tropical cyclogenesis in the western north pacific for 2000 and 2001. *Wea. Forecasting*, **22**, 763–780.
- Hendricks, E. A., M. T. Montgomery, and C. A. Davis, 2004: The role of vortical hot towers in the formation of tropical cyclone diana (1984). *J. Atmos. Sci.*, **61**, 1209–1232.
- Hoxit, L. R., C. Chappell, and J. Fritch, 1976: Formation of mesolows or pressure troughs advance of cumulonimbus clouds. *Mon. Wea. Rev.*, **104**, 1419–1428.
- Kieu, C. Q. and D.-L. Zhang, 2009: Genesis of tropical storm eugene (2005) from merging vortices associated with itcz breakdowns. part ii: Roles of vortex merger and ambient potential vorticity. *J. Atmos. Sci.*, **66**, 1980–1996.

- Li, T. and B. Fu, 2006: Tropical cyclogenesis associated with rossby wave energy dispersion of a preexisting typhoon. part i: Satellite data analyses. *J. Atmos. Sci.*, **63**, 1377–1389.
- Miyoshi, T. and M. Kunii, 2012: The local ensemble transform kalman filter with the weather research and forecasting model: Experiments with real observations. *Pure Appl. Geophys.*, **169**, 321–333.
- Montgomery, M. T., M. E. Nicholls, T. A. Cram, and A. B. Saunders, 2006: A vortical hot tower route to tropical cyclogenesis. *J. Atmos. Sci.*, **63**, 355–386.
- Rappaport, E. N. and J. Franklin, 2009: Advances and challenges at the national hurricane center. *Wea. Forecasting*, **24**, 395–419.
- Reynolds, R. W., T. M. Smith, C. Lui, D. B. Chelton, K. S. Casey, and M. G. Schlax, 2007: Daily high-resolution blended analyses for sea surface temperature. *J. Climate*, **20**, 5473–5496.
- Ritchie, E. A. and G. J. Holland, 1997: Scale interactions during the formation of typhoon irving. *Mon. Wea. Rev.*, **125**, 1377–1396.
- Simpson, J., J. B. Halverson, B. S. Ferrier, W. A. Petersen, R. H. Simpson, R. Blakeslee, and S. L. Durden, 1998: On the role of "hot towers" in tropical cyclone formation. *Meteor. Atmos. Phys.*, **67**, 15–35.
- Sippel, J. A. and F. Zhang, 2008: The probabilistic analysis of the dynamics and predictability of tropical cyclogenesis. *J. Atmos. Sci.*, **65**, 3440–3459.
- Snyder, A. D., Z. Pu, and Y. Zhu, 2010: Tracking and verification of east atlantic tropical

- cyclone genesis in the ncep global ensemble: Case studies during the nasa african monsoon multidisciplinary analyses. *Wea. Forecasting*, **25**, 1397–1411.
- Trenberth, K. E., 1986: An assessment on the impact of transient eddies on the zonal flow during a blocking episode using the localized Eliassen-Palm flux diagnostics. *J. Atmos. Sci.*, **43**, 2070–2087.
- Vizy, E. K. and K. H. Cook, 2009: Tropical storm development from African easterly waves in the eastern Atlantic: A comparison of two successive waves using a regional model as part of NASA Aamma 2006. *J. Atmos. Sci.*, **66**, 3313–3334.
- Wang, Z., M. T. Montgomery, and T. J. Dunkerton, 2010a: Genesis of prehurricane Felix (2007). part i: The role of the easterly wave critical layer. *J. Atmos. Sci.*, **67**, 1711–1729.
- Zhang, D.-L. and N. Bao, 1996b: Oceanic cyclogenesis as induced by a mesoscale convective system moving offshore. part ii: Genesis and thermodynamic transformation. *Mon. Wea. Rev.*, **124**, 2206–2226.
- Zhang, D.-L. and H. Chen, 2012: Importance of the upper-level warm core in the rapid intensification of tropical cyclone. *Geophys. Res. Lett.*, **39**, 2806–2812.
- Zisper, E. J. and C. Gautier, 1978: Mesoscale events within a gate tropical depression. *Mon. Wea. Rev.*, **106**, 789–805.

## List of Figures

- 1    Hovmoller Diagram of 700 hPa relative vorticity from ERA–Interim data. The solid arrow represents the progression of the wave that becomes Hurricane Julia, the storm of interest. The dashed arrow represents the storm prior to Hurricane Julia, Hurricane Igor. The dashed horizontal line represents the initialization time of the WRF control simulation. 32
  
- 2    Setup of the WRF simulation at the initialization time of 0000 UTC 10 Sept. The ERA–Interim 700 hPa streamlines are shown with NOAA OI SSTs shaded. The boxes represent the domains of the WRF simulation, with the moving nest (smallest boxes) following the disturbance that becomes Hurricane Julia. 33
  
- 3    METEOSAT-9 IR (left) compared with WRF control simulation OLR (shaded) and 850 hPa streamlines on the right. Images show critical times in the disturbance’s evolution, with the last image set being TD declaration (0600 UTC 12 Sept). 34
  
- 4    Comparisons of NHC best track estimates for track (a) and intensity (b). (a) Shows the observed track (black) versus the WRF control simulation track (gray). The average track error between the two was approx. 193km. (b) Shows the intensity comparison for minimum central pressure ( $P_{MIN}$ , solid lines) and maximum 10m wind speed ( $V_{MAX}$ , dashed lines) for the observed (black) and WRF control (gray). 35

- 5 WRF simulation 700 hPa relative vorticity (shaded) and co-moving stream-  
lines. Phase speed for the storm ( $C_p$ ) was estimated as just over  $6.5 \text{ m s}^{-1}$   
and co-moving streamlines are plotted as  $V_{co-moving} = V - C_p$ . 36
- 6 Dakar (GOOY) soundings as the AEW passed over the rawinsonde station.  
Strong easterly flow between 925 and 700 hPa is noted during its passage. 37
- 7 WRF simulation 925-600 hPa (left) and 600-200 hPa (right) layer-averaged  
RH (shaded) and wind shear barbs. Sufficient column moisture exists in the  
lower troposphere, but struggles to reach the middle and upper troposphere. 38
- 8 WRF simulation 1000 hPa relative vorticity (shaded) and streamlines. “1”  
and “2” represent the northern and southern vortex respectively, while “V”  
represents the merged vortex. The red line represents the cross-section used  
in later figures for 0600 UTC 11 Sept. 39
- 9 WRF simulation temperature deviation cross-section from 1000 to 200 hPa  
through both near-surface vortexes. B represents the beginning of the cross-  
section and E represents the end. 3D wind vectors are also plotted in black  
at various pressure levels. 40
- 10 WRF simulation cross-section of relative humidity (shaded) and 3D wind  
vectors in the 1000 to 700 hPa layer. B and E represent the same as in Fig. 9. 41
- 11 WRF simulation T-T0 where T0 is the temperature at the initial time for the  
point of TCG and potential temperature (contours). The upper-level warm  
core develops between 8 and 12 km, becoming most prominent 24 h before  
genesis occurs. 42

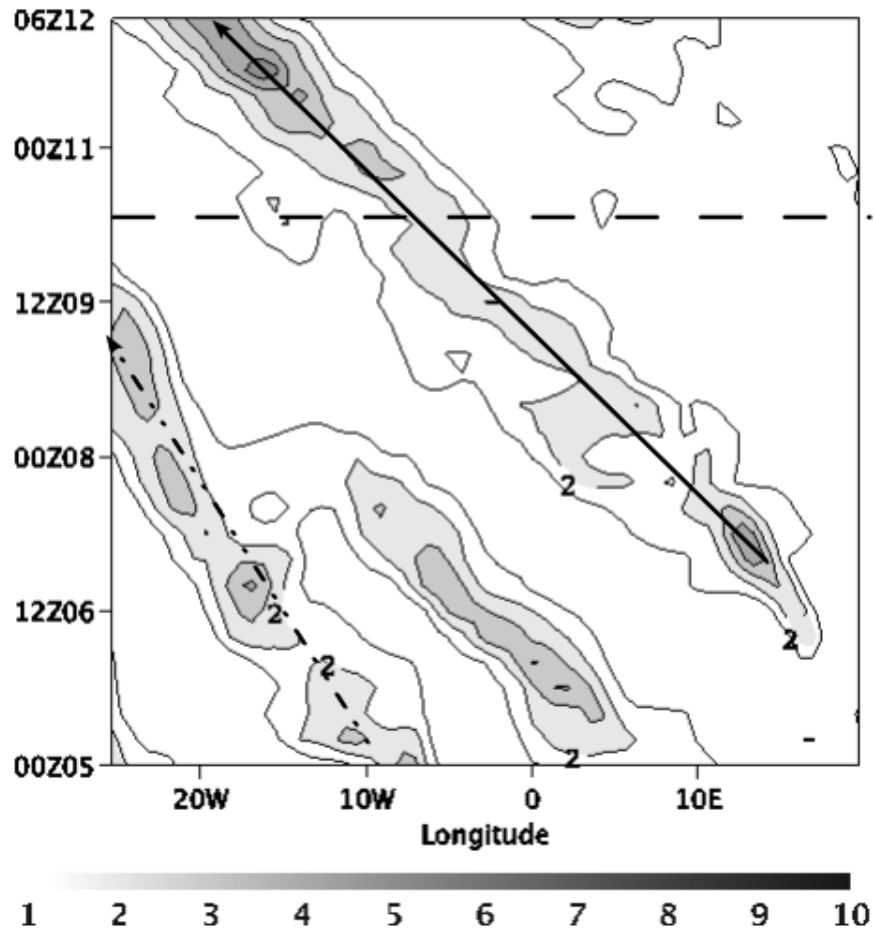


FIG. 1. Hovmoller Diagram of 700 hPa relative vorticity from ERA-Interim data. The solid arrow represents the progression of the wave that becomes Hurricane Julia, the storm of interest. The dashed arrow represents the storm prior to Hurricane Julia, Hurricane Igor. The dashed horizontal line represents the initialization time of the WRF control simulation.

0000 UTC 10 Sept 2010

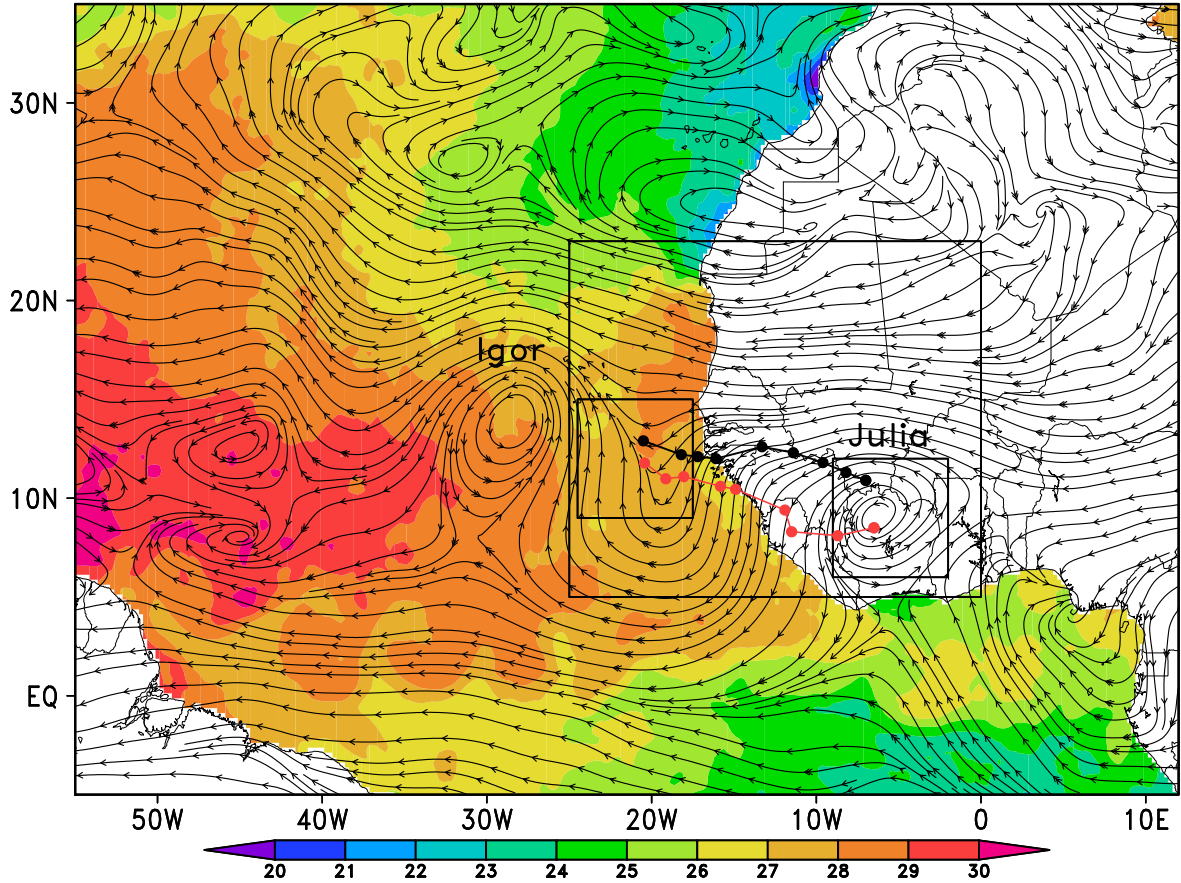


FIG. 2. Setup of the WRF simulation at the initialization time of 0000 UTC 10 Sept. The ERA-Interim 700 hPa streamlines are shown with NOAA OI SSTs shaded. The boxes represent the domains of the WRF simulation, with the moving nest (smallest boxes) following the disturbance that becomes Hurricane Julia.

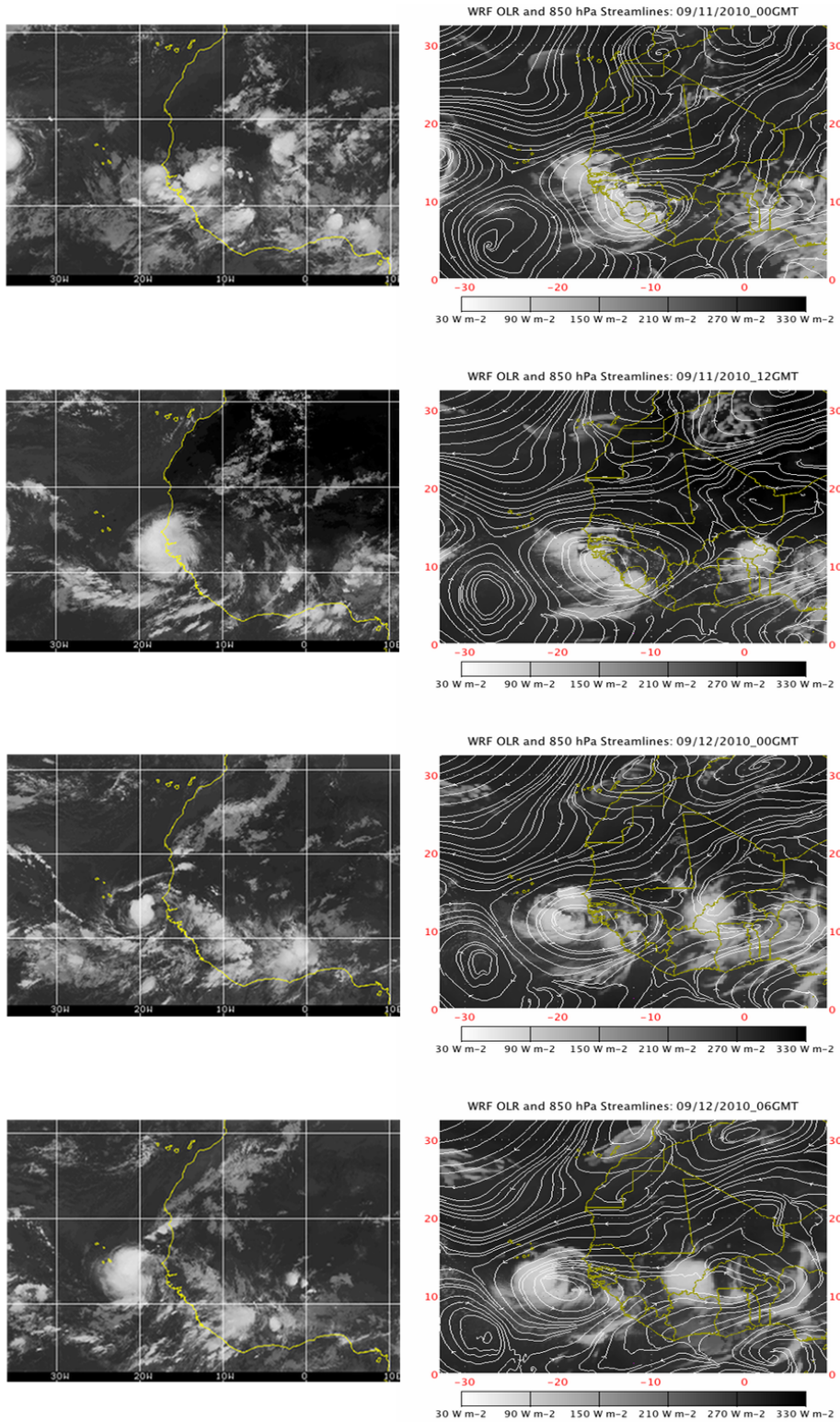


FIG. 3. METEOSAT-9 IR (left) compared with WRF control simulation OLR (shaded) and 850 hPa streamlines on the right. Images show critical times in the disturbance's evolution, with the last image set being TD declaration (0600 UTC 12 Sept).

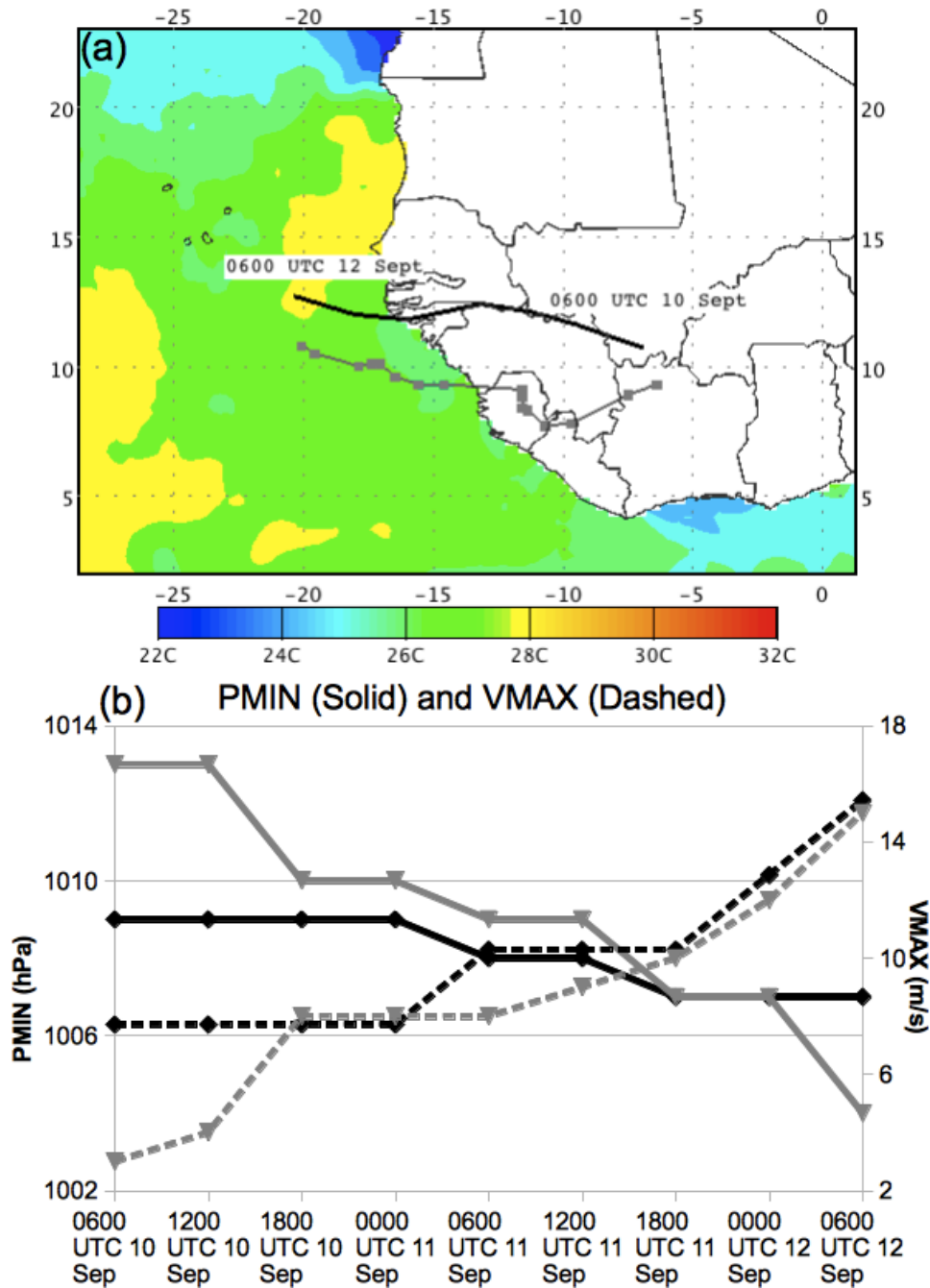


FIG. 4. Comparisons of NHC best track estimates for track (a) and intensity (b). (a) Shows the observed track (black) versus the WRF control simulation track (gray). The average track error between the two was approx. 193km. (b) Shows the intensity comparison for minimum central pressure ( $P_{MIN}$ , solid lines) and maximum 10m wind speed ( $V_{MAX}$ , dashed lines) for the observed (black) and WRF control (gray).

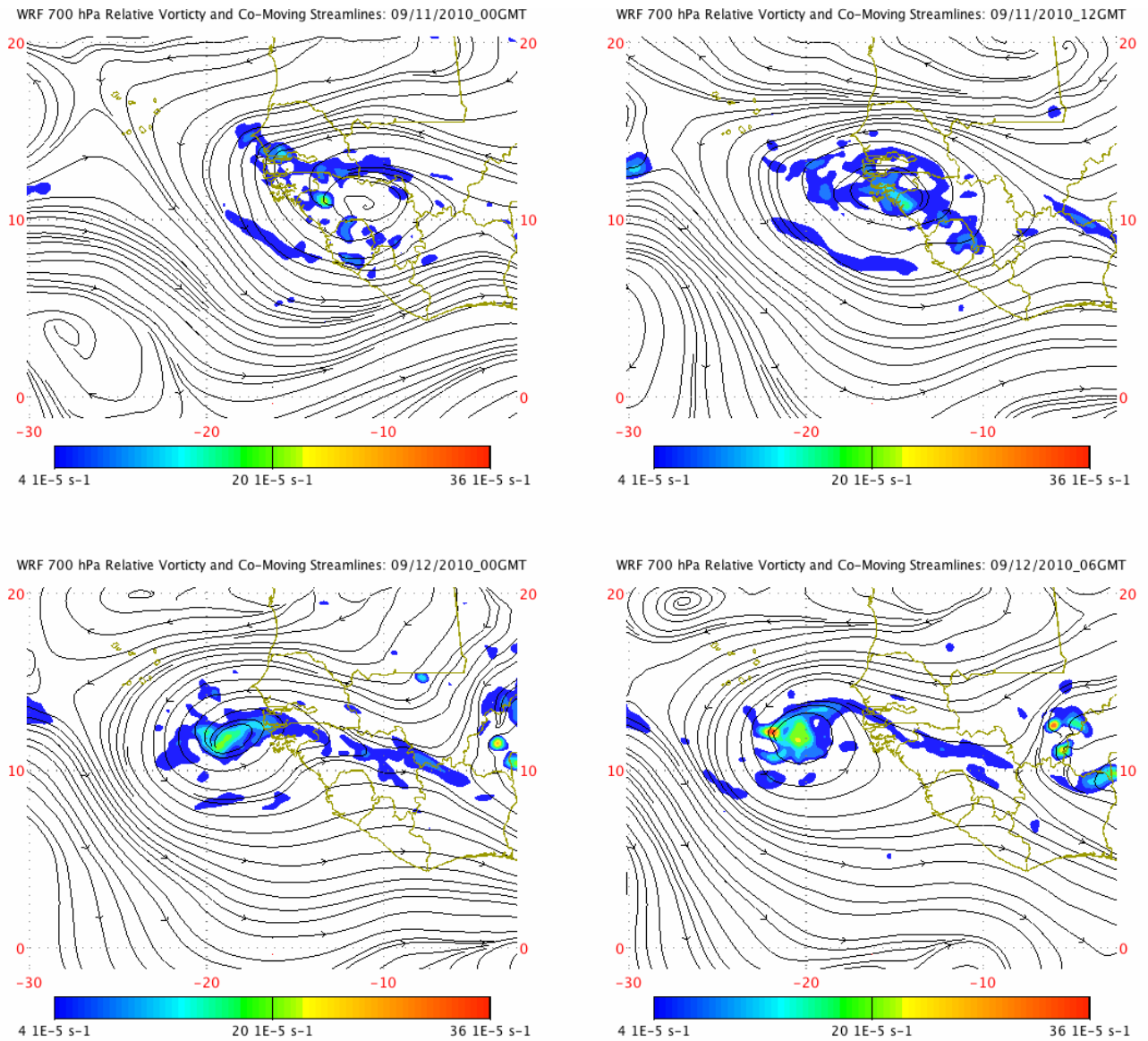


FIG. 5. WRF simulation 700 hPa relative vorticity (shaded) and co-moving streamlines. Phase speed for the storm ( $C_p$ ) was estimated as just over  $6.5 \text{ m s}^{-1}$  and co-moving streamlines are plotted as  $V_{co-moving} = V - C_p$ .

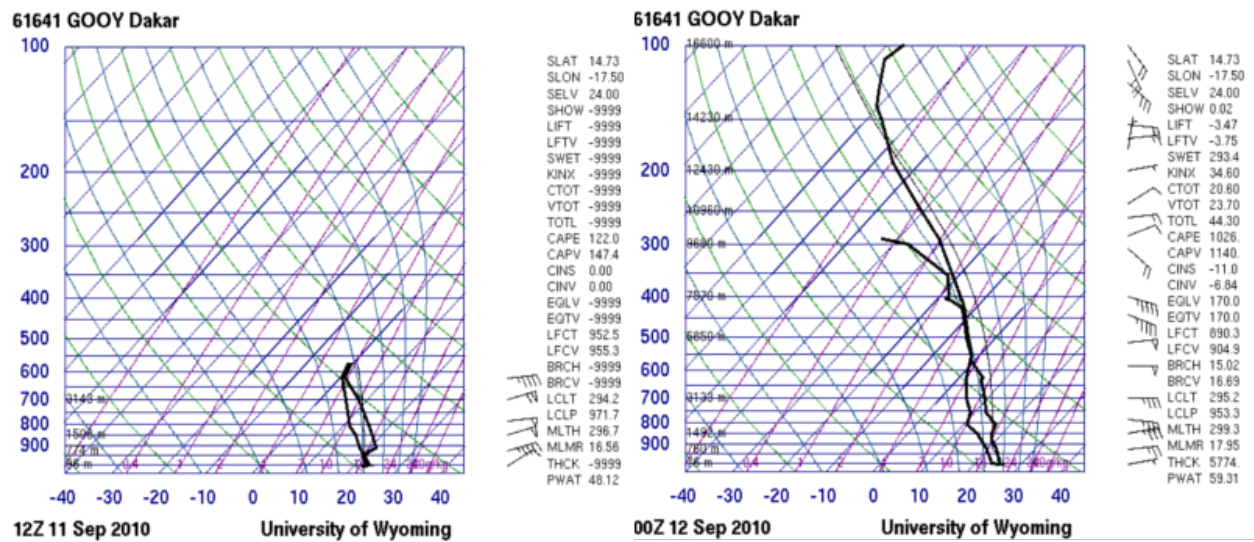


FIG. 6. Dakar (GOOY) soundings as the AEW passed over the rawinsonde station. Strong easterly flow between 925 and 700 hPa is noted during its passage.

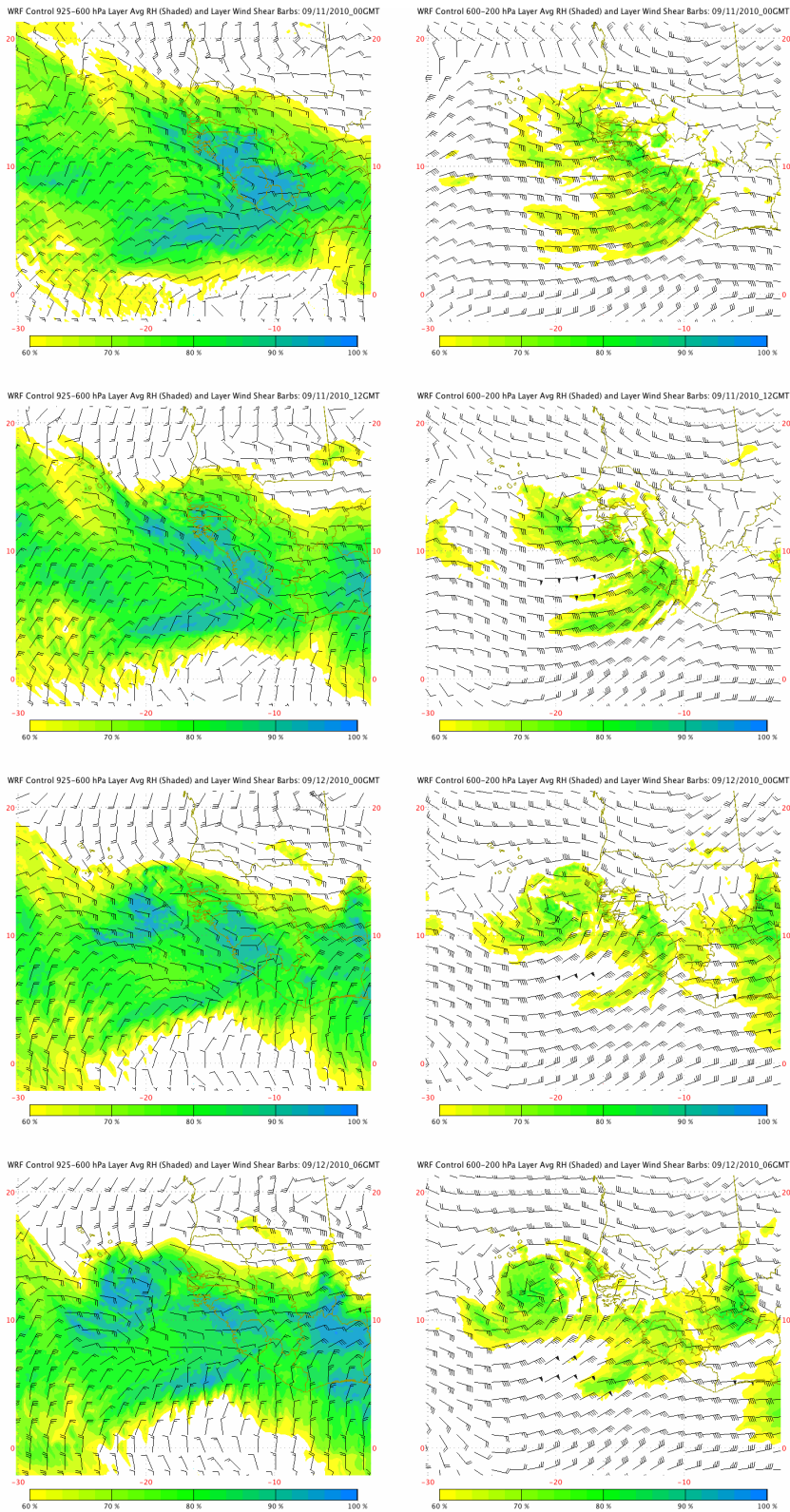


FIG. 7. WRF simulation 925-600 hPa (left) and 600-200 hPa (right) layer-averaged RH (shaded) and wind shear barbs. Sufficient column moisture exists in the lower troposphere, but struggles to reach the middle and upper troposphere.

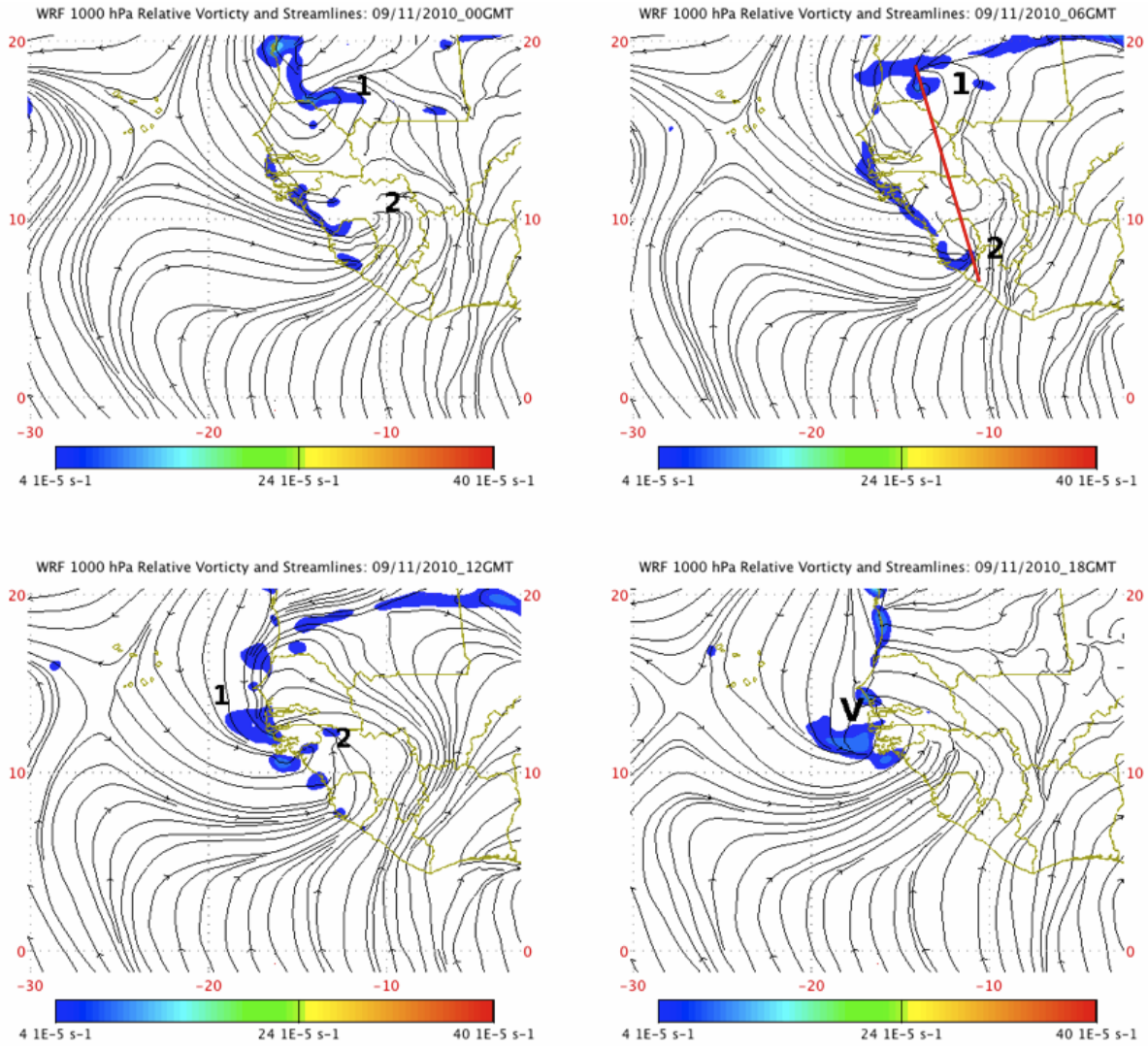


FIG. 8. WRF simulation 1000 hPa relative vorticity (shaded) and streamlines. “1” and “2” represent the northern and southern vortex respectively, while “V” represents the merged vortex. The red line represents the cross-section used in later figures for 0600 UTC 11 Sept.

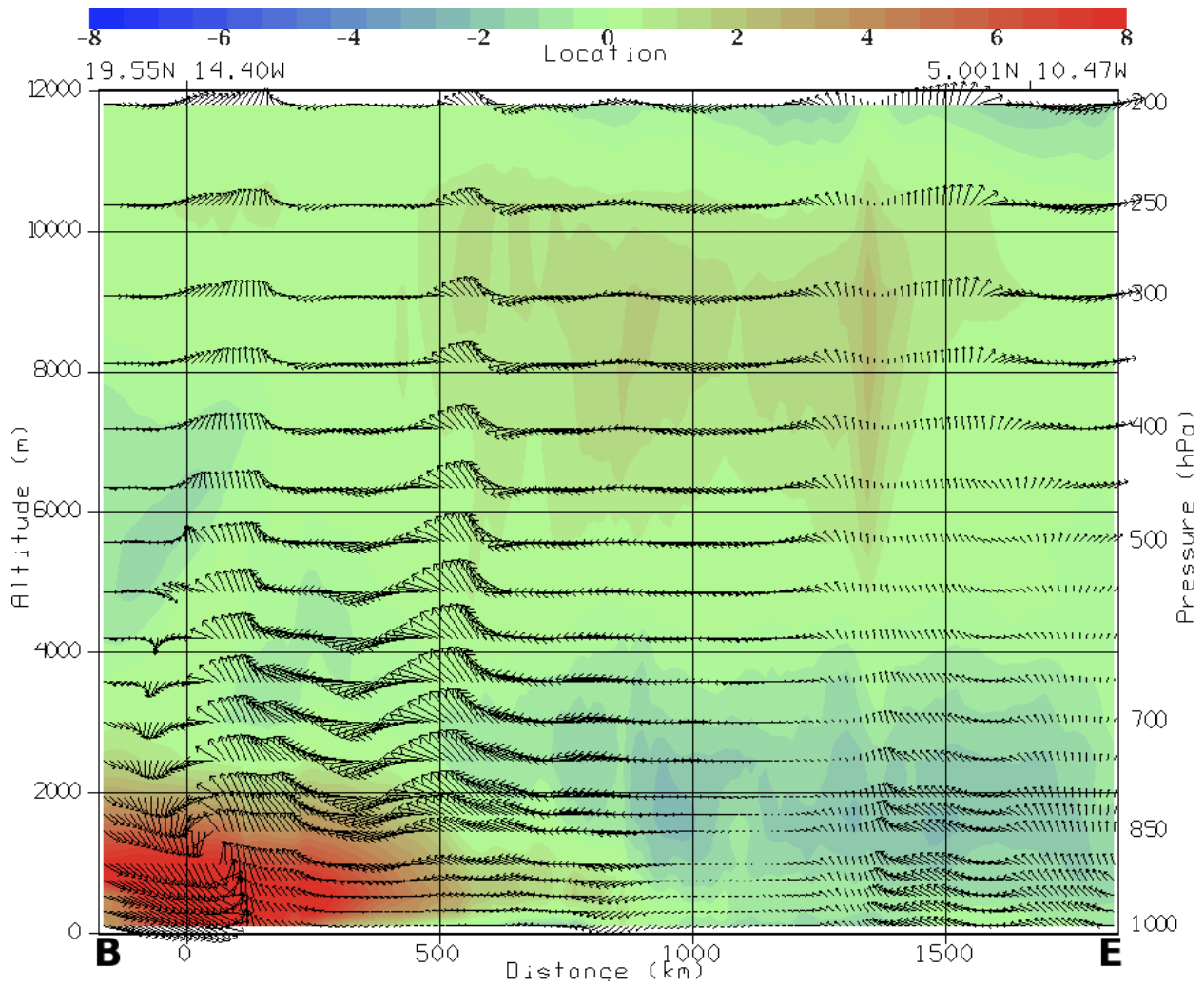


FIG. 9. WRF simulation temperature deviation cross-section from 1000 to 200 hPa through both near-surface vortices. B represents the beginning of the cross-section and E represents the end. 3D wind vectors are also plotted in black at various pressure levels.

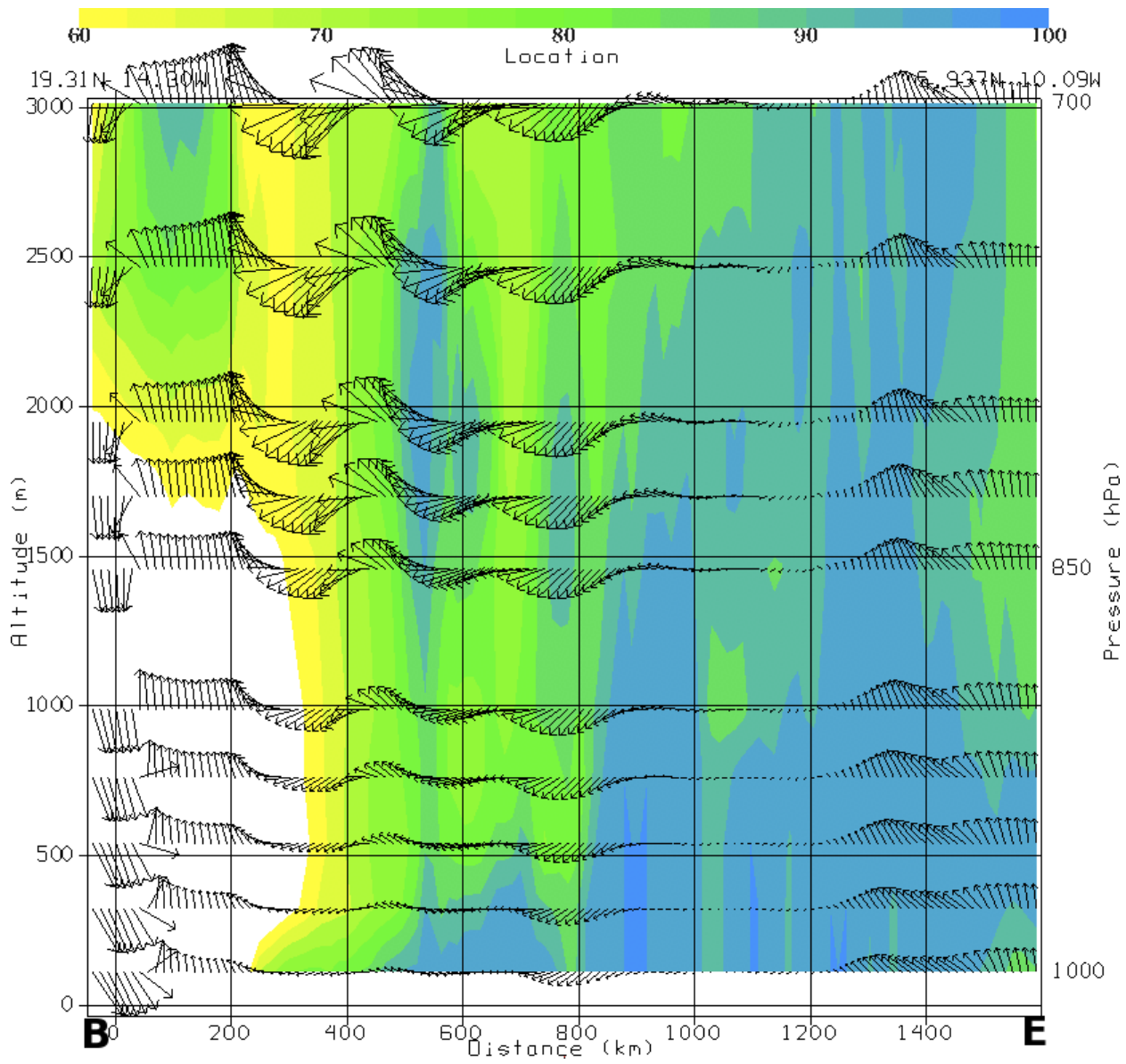


FIG. 10. WRF simulation cross-section of relative humidity (shaded) and 3D wind vectors in the 1000 to 700 hPa layer. B and E represent the same as in Fig. 9.

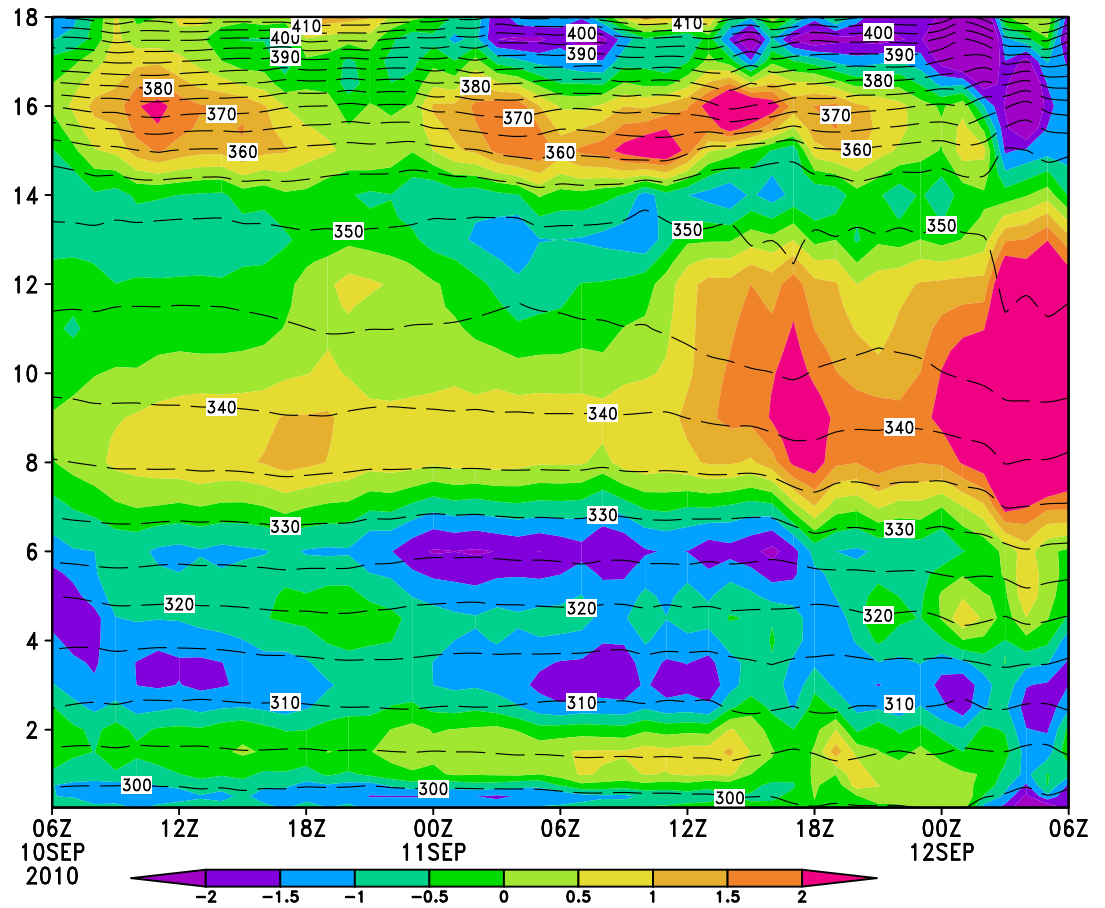


FIG. 11. WRF simulation  $T-T_0$  where  $T_0$  is the temperature at the initial time for the point of TCG and potential temperature (contours). The upper-level warm core develops between 8 and 12 km, becoming most prominent 24 h before genesis occurs.